Acta Oceanol. Sin., 2018, Vol. 37, No. 5, P. 67–76
DOI: 10.1007/s13131-018-1212-6
http://www.hyxb.org.cn
E-mail: hyxbe@263.net

Impacts of changing scale on Getis-Ord Gi* hotspots of CPUE: a case study of the neon flying squid (*Ommastrephes bartramii*) in the northwest Pacific Ocean

FENG Yongjiu[1, 2, 3, 4], CHEN Xinjun[1, 3, 4*], GAO Feng[1, 3, 4], LIU Yang[1]

[1] College of Marine Sciences, Shanghai Ocean University, Shanghai 201306, China

[2] Laboratory for Marine Fisheries Science and Food Production Processes, Qingdno National Laboratory for Marine Science and Technology, Qingdao 266235, China

[3] National Distant-water Fisheries Engineering Research Center, Shanghai Ocean University, Shanghai 201306, China

[4] Key Laboratory of Sustainable Exploitation of Oceanic Fisheries Resources (Shanghai Ocean University), Ministry of Education, Shanghai 201306, China

Received 6 December 2016; accepted 5 February 2017

Abstract

We examined the scale impacts on spatial hot and cold spots of CPUE for *Ommastrephes bartramii* in the northwest Pacific Ocean. The original fishery data were tessellated to 18 spatial scales from 5′×5′ to 90′×90′ with a scale interval of 5′ to identify the local clusters. The changes in location, boundaries, and statistics regarding the Getis-Ord Gi* hot and cold spots in response to the spatial scales were analyzed in detail. Several statistics including Min, mean, Max, SD, CV, skewness, kurtosis, first quartile (Q1), median, third quartile (Q3), area and centroid were calculated for spatial hot and cold spots. Scaling impacts were examined for the selected statistics using linear, logarithmic, exponential, power law and polynomial functions. Clear scaling relations were identified for Max, SD and kurtosis for both hot and cold spots. For the remaining statistics, either a difference of scale impacts was found between the two clusters, or no clear scaling relation was identified. Spatial scales coarser than 30′ are not recommended to identify the local spatial patterns of fisheries because the boundary and locations of hot and cold spots at a coarser scale are significantly different from those at the original scale.

Key words: *Ommastrephes bartramii*, scale impacts, local clusters, Getis-Ord Gi*, spatial hotspots

Citation: Feng Yongjiu, Chen Xinjun, Gao Feng, Liu Yang. 2018. Impacts of changing scale on Getis-Ord Gi* hotspots of CPUE: a case study of the neon flying squid (*Ommastrephes bartramii*) in the northwest Pacific Ocean. Acta Oceanologica Sinica, 37(5): 67–76, doi: 10.1007/s13131-018-1212-6

1 Introduction

Spatial patterns of marine and estuarial fisheries are important geographic observations that can benefit sustainable exploration (Feng et al., 2017a; Huang et al., 2014; Jiang et al., 2016) and provide managers with the best information for responsible and responsive management (Cope and Punt, 2011). These patterns are usually in the form of a spatiotemporal distribution and its relationships with oceanic environments (Chen et al., 2014; Jennings et al., 2009; Swartz et al., 2010; Yu et al., 2015). They are commonly analyzed using integrated geographic information systems (GIS), spatial analysis, geostatistics and remote sensing (Carocci et al., 2009; Meaden and Aguilar-Manjarrez, 2013). The spatiotemporal distribution of fisheries resources has been investigated extensively for offshore and pelagic species such as *Ommastrephes bartramii*, *Dosidicus gigas*, *Lophelia pertusa*, *Chaceon notialis*, and *Thunnus albacares* (Chen and Chiu, 2003; Chen et al., 2008; Feng et al., 2017b; Fosså et al., 2002; Gilly et al., 2006; Gutiérrez et al., 2011; Nishida and Chen, 2004; Paulino et al., 2016; Yu et al., 2016a). These studies have made a substantial contribution towards understanding spatial distribution and aggregation of fisheries and resolution of spatial problems of fisheries and aquaculture worldwide.

Spatial patterns in fisheries are commonly analyzed on a specified grid where the original data have been tessellated to a regularly-defined spatial scale. In some case studies, original and un-tessellated fishery data at a very coarse scale were used to analyze the spatial patterns of pelagic species (Feng et al., 2017c; Su et al., 2008). Feng et al. (2017a) identified the spatial variability of *O. bartramii* in the northwest Pacific Ocean at original scales, while Su et al. (2008) examined the relationship between spatiotemporal patterns of blue marlin (*Makaira nigricans*) in the Pacific Ocean on a 5°×5° coarse scale. A spatial scale of 30′×30′ is the most widely used fishing grid for investigating the distribution of commercial fisheries such as *O. bartramii* and *D. gigas* (Chen et al., 2008; Yu et al., 2016b). For example, Chen et al. (2008) conducted a stock assessment at a 30′×30′ scale to spatially estimate stock size and proportional escapement of *O. bartramii* in the northwest Pacific Ocean. On the same scale, Xu et al. (2016) examined the effect of sea surface temperature increase on the potential habitat of *O. bartramii* in the Northwest

Foundation item: The National Natural Science Foundation of China under contract No. 41406146; the Open Fund from Laboratory for Marine Fisheries Science and Food Production Processes at Qingdao National Laboratory for Marine Science and Technology of China under contract No. 2017-1A02; Shanghai Universities First-class Disciplines Project-Fisheries (A).
*Corresponding author, E-mail: xjchen@shou.edu.cn

Pacific Ocean; Yu et al. (2016b) evaluated the effects of climate variability on habitat suitability of *D. gigas* over the 2006–2012 period in the sea waters offshore Peru. Finer scales have commonly been used to examine spatial patterns of fisheries in coastal waters. Saul et al. (2013) explored the spatial distribution of reef fish and estimated their spatial autocorrelation at a spatial scale of 10′×10′ on the West Florida Shelf. Using the same spatial resolution of 10′×10′, Gao et al. (2016) built a boosted regression trees-based model to forecast fishing ground of *Scomber japonicus* in the Yellow Sea and East China Sea. At a much finer 1 km×1 km spatial scale, Harford et al. (2015) simulated scenarios representing spiny lobster distribution at Glover's Reef Marine Reserve, Belize.

Spatial patterns at one scale may not be valid at a different scale (Wu, 2004) and mismatch of model spatial scale and biological stock structure may compromise management goals (Cope and Punt, 2011), because the patterns and structures differ from scale to scale (Feng and Liu, 2015). This phenomenon has been recognized as "scale impact" or "scale effect" (Turner et al., 1989; Wiens, 1989). Tian et al. (2010) noted the scale impact on catch-per-unit-effort (CPUE) standardization and conducted a case study using the commercial fishery data of *O. bartramii* and the corresponding oceanographic data in the northwest Pacific Ocean. They tessellated the fishery data into 0.5°, 1°, 2°, 3°, 4° and 5° scales and showed that spatial scale significantly affected the standardization of CPUE. Using a similar tessellation scheme, Gong et al. (2014) evaluated the effects of spatial scale on habitat suitability modeling for *O. bartramii* in the northwest Pacific Ocean. They noted that a scale such as 30′ is too large and may compromise the reliability of modelling and miss significant details of the scaling relations. Research has also showed that the changing spatial scales may substantially affect the observed spatial patterns for fisheries resources (Guinet et al., 2001; Yang et al., 2013).

We have conducted a quantitative evaluation of the scale effect on several spatial indices in analyzing the observed patterns of *O. bartramii* resources in the northwest Pacific Ocean (Feng et al., 2016). These spatial indices included global Moran's I index, Geary's C, Getis-Ord General G, the average nearest neighbor (ANN) and Ripley's K function. These indices were focused on the examination of global patterns in terms of clustering, dispersal and random distribution of fisheries. We proposed trend and extent indicators that quantify the scale impacts of the spatial indices. Based on spatial autocorrelation statistics Moran's I and Geary's C, we identified 25′×25′ as the optimum scale for August and October and 20′×20′ as the optimum scale for September in conducting spatial analyses of *O. bartramii* in the northwest Pacific Ocean. We also identified 50′×50′ as the coarsest allowable spatial scale for August and October and 50′×50′ as the coarsest allowable spatial scale for September. The optimum and coarsest allowable spatial scales changed by month since the scaling effects depend on monthly different commercial fishery data.

This paper extends early study of Feng et al. (2016) and examines the scale impact of on local spatial clusters using the same fishery dataset of *O. bartramii*. There are three major differences between the earlier study and the present paper, which are as follows: (1) the early study investigated the scale impacts of the *global* patterns while the present paper examines the scale impacts of the *local* patterns, (2) the global indices of spatial relationships were calculated in the earlier study while the summary statistics within the *local* clusters are computed in the present paper, and (3) the early study examined a vast of spatial indices while the present paper focuses on the spatial hotspots derived from Getis-Ord Gi*. Specifically, the hot and cold spots at various spatial scales were identified and changes in their locations, boundaries and statistics in relation to spatial scales were studied in more detail. In examining scale impacts, we selected a number of spatial and non-spatial indices including Min, mean, Max, SD, CV, skewness, kurtosis, first quartile (Q1), median, third quartile (Q3), area and centroid. Our study examines the relationships between hot/cold spots and spatial scale. Our results contribute to enhancing our understanding of the relationships between spatial scale and local spatial clusters of fisheries, and to the selection of an appropriate spatial scale for analysis of fisheries.

2 Materials and methods

2.1 *Commercial fishery data*

Commercial fishery data of *O. bartramii* in the northwest Pacific Ocean were collected by the Chinese Squid-jigging Technology Group (CSTG). The data include the dates of fishing, fishing locations (longitude and latitude), the number of fishing vessels operating per day, and daily catch of vessels. The commercial fishing data of *O. bartramii* were selected within the boundary of 38°–46°N and 150°–162°E. In this paper, we focused on Chinese Mainland fisheries of *O. bartramii* in August, September and October from 2004 to 2013 and examined their scale impacts on the hot and cold spots of this squid fishery.

Examination of the scale impacts on local clusters was conducted using CPUE data. The CPUE at each vessel location was calculated as the total catches divided by the number of fishing operations at the location:

$$CPUE_j = \frac{\sum_{i=1}^{10} C_{i,j,ss}}{\sum_{i=1}^{10} E_{i,j,ss}}, \tag{1}$$

where $C_{i,j,ss}$ is the catch (t) in month j year i within a fishing grid (spatial scale, SS), and $E_{i,j,ss}$ is the number of the corresponding fishing operations (efforts) in month j year i within the same fishing grid.

The spatial scale of the original data was assessed using the ANN method (Ebdon, 1985; Mitchell, 2005). The estimated spatial scales of the original datasets are 1.07′ for August, 0.94′ for September and 0.99′ for October (Feng et al., 2016). These original datasets were then tessellated to 18 spatial scales from 5′×5′ to 90′×90′, with a scale interval of 5′ between two adjacent spatial scales. We therefore used a total of 19 spatial scales for multi-scale analysis, including the original dataset. Figure 1 illustrates the original fishery data and the datasets that were tessellated at 30′×30′, 60′×60′ and 90′×90′ spatial scales.

2.2 *Hot and cold spots*

Global spatial autocorrelation methods such as Getis-Ord General G measure the overall clustering or dispersion pattern of fishing grounds (Feng et al., 2017a). In contrast, local spatial autocorrelation statistics (Getis and Ord, 1996; Ord and Getis, 1995; Peeters et al., 2015) are commonly used to investigate the specific spatial distribution and local clusters of fisheries (Feng et al., 2017a). Getis-Ord Gi* is one of the most widely used local spatial autocorrelation statistics, and is given by (Getis and Ord, 1996; Ord and Getis, 1995):

$$Gi^* = \frac{\sum_{j=1}^{n} w_{i,j}x_j - \bar{X}\sum_{j=1}^{n} w_{i,j}}{S \times \sqrt{\left(n\sum_{j=1}^{n} w_{i,j}^2 - \left(\sum_{j=1}^{n} w_{i,j}\right)^2\right)/(n-1)}}, \tag{2}$$

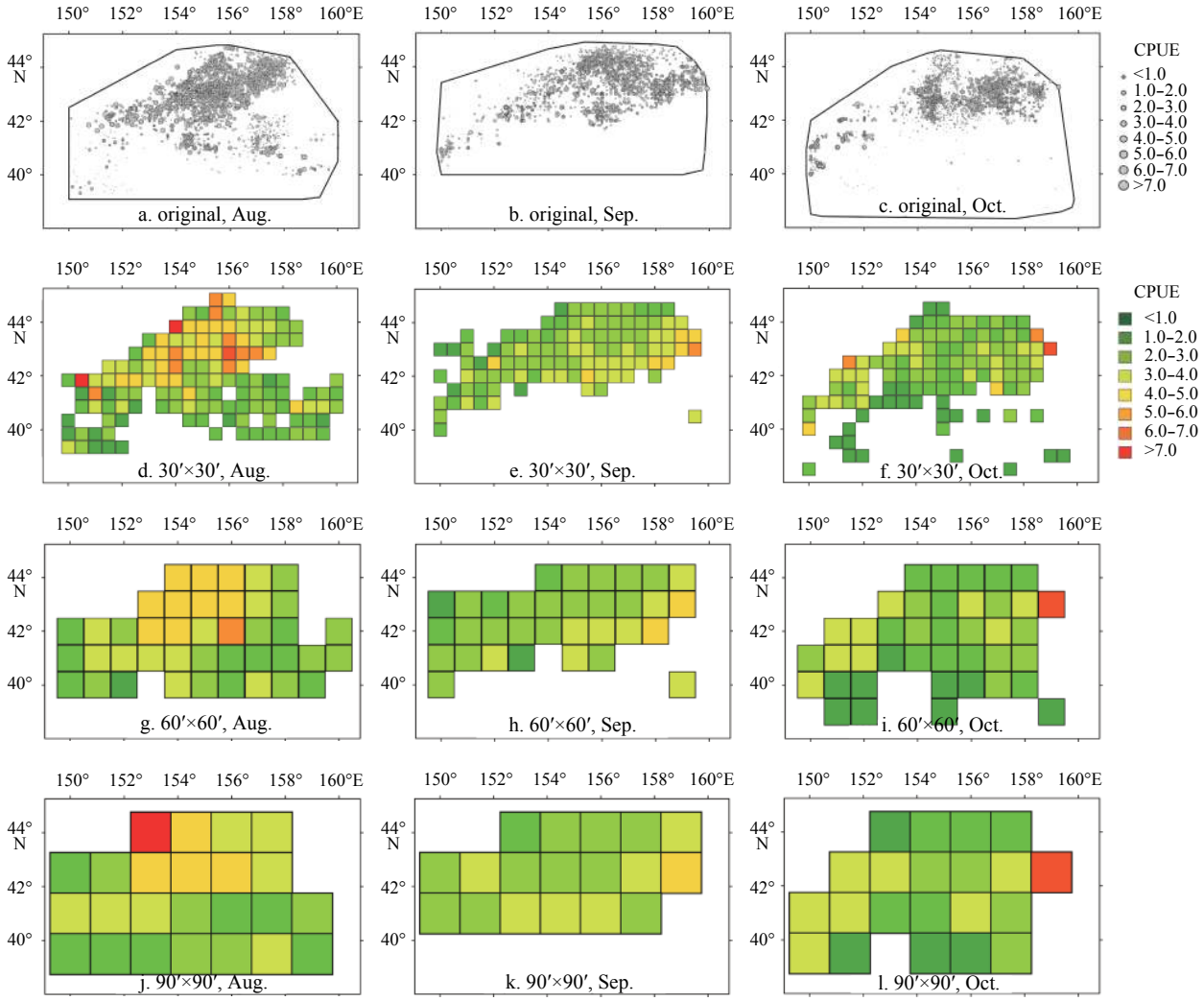

Fig. 1. Original fishery data and tessellated fishery data at 30′×30′, 60′×60′ and 90′×90′.

where S is the standard deviation of all data points, n is the number of data points, x_j is the CPUE of points j, $\bar{X}$ is the averaged value of all points, and $w_{i,j}$ is the spatial weights matrix indicating the spatial adjacency relations between the point (i) in processing and the neighboring point j. Generally, the spatial weight matrix $w_{i,j}$ is defined by using either an adjacency standard or a distance standard (Getis and Aldstadt, 2010).

In practice, Getis-Ord Gi* statistics return two values: (1) the z-score of each point, and (2) the consequent significance p-value. At 5% significance, a z-score greater than 2 indicates a hot spot while a z-score smaller than –2 indicates a cold spot. A hot spot signifies that the data points with high CPUE values are surrounded by similarly high CPUE points, whereas a cold spot signifies that points with low CPUE are surrounded by similarly low CPUE points. This indicates that both hot and cold spots are spatial clusters in the fishery. A z-score between –1 and 1 indicates that the underlying pattern probably results from random spatial processes (Feng et al., 2017a). In our study, the hot and cold spots of *O. bartramii* in the northwest Pacific Ocean were identified using Getis-Ord Gi* in ArcGIS 10.1.

2.3 *Measured indices*

Several spatial and non-spatial indices were selected to measure the spatial distribution of CPUE for *O. bartramii* and then to examine any scale impacts. We used indices such as summary statistics including Min, mean, Max, SD, CV, skewness, kurtosis, Q1, median, and Q3 as well as spatial measurements such as area and centroid. Spatial hot and cold spots in the fishery were identified by Getis-Ord Gi*, a widely used local spatial autocorrelation statistic (Getis and Aldstadt, 2010; Getis and Ord, 1996; Ord and Getis, 1995). Hot and cold spots on different spatial scales were identified and the changes in their locations, boundaries, and statistics resulting from the changes in spatial scales were studied in detail.

2.4 *Measuring the scale impacts*

The scale impacts of the indices were assessed by regression modelling using linear, power law, logarithmic, exponential, and polynomial functions (Table 1), drawing references from the literature in landscape ecology (Feng and Liu, 2015; Turner et al., 1989; Wu, 2004).

In Table 1, y is the spatial index and x is the spatial scale. For linear, logarithmic and exponential functions, positive a indicates a growing trend of an index while a negative a indicates a decaying trend as the spatial scale increases. The sign of a is a trend indicator. For power law functions, the fractal dimension d quantifies the scale extent according to earlier works (Feng and Liu, 2015), where d=–1–a (a>0) or d=1–a (a<0). Negative d (a>0) in-

Table 1. Potential scale impacts of indices in analyzing fisheries resources

Scaling relations	Equation	Meaning
Linear	$y=ax+b$	$a>0$ means that the index increases as spatial scale (fish grid) becomes coarser, i.e., a growing trend, whereas $a<0$ means that the index decreases as the spatial scale becomes coarser, i.e., a decaying trend.
Logarithmic	$y=a\ln x+b$	
Exponential	$y=a+be^{cx}$	
Power law	$y=bx^a$	
Polynomial	$y=a_nx^n+\ldots+a_1x+a_0$, $n\geqslant 2$	$n=2$ indicates a parabolic curve, while $n>2$ indicates a more complex relationship between a spatial index and the corresponding spatial scales.

dicates that the spatial index increases as the spatial scale becomes coarser (i.e., a larger grid size), whereas a positive d ($a<0$) indicates that the spatial index decreases as the spatial scale becomes coarser. The dimension $|d|$ approaching 1 means that the spatial index is not sensitive to the change of the spatial scale, whereas large $|d|$ (e.g., $|d|\geqslant 1.3$) means that the spatial index is sensitive to the change of the spatial scale (Feng and Liu, 2015; Wu, 2004).

3 Results

3.1 *The distribution of O. bartramii CPUE at 30′*

Each fishery data in this study corresponds to 19 spatial scales, leading to a total of 57 datasets for all three months. We therefore analyzed the distribution of CPUE under a widely applied spatial scale of 30′ (Fig. 2). There are 136, 101 and 107 fishing points and their mean values are 2.89, 2.69 and 2.12 for August, September and October, successively. The standard deviation ranges from 1.05 to 1.59, suggesting relatively aggregation distribution of the CPUE data. Figure 2 shows that the CPUE yield leptokurtic distribution for all three months, indicating low variations of *O. bartramii* CPUE across space. These CPUE datasets are therefore suitable for identifying the spatial hot and cold spots using local Getis-Ord Gi* statistic.

3.2 *Scale impacts on summary statistics of entire dataset*

The summary statistics for CPUE in the study area did not exhibit any clear scaling relations except Max and CV, as illustrated by scaling equations, the associated goodness-of-fit R^2s (Table 2) and the scaling curves (Fig. 3). This means that most of the summary statistics varied with a change in spatial scale. Both Max and CV showed exponential scaling relations with decaying trends for August and September, which may be due to the fact that the calculated CPUE is the averaged value of all data points within a fishing grid. The two statistics yielded double-quadratic polynomials that open upward for October. The 55′ scale defines the break point in the two quadratic polynomials for both Max and CV, and the early stages of Max and CV show decaying trends

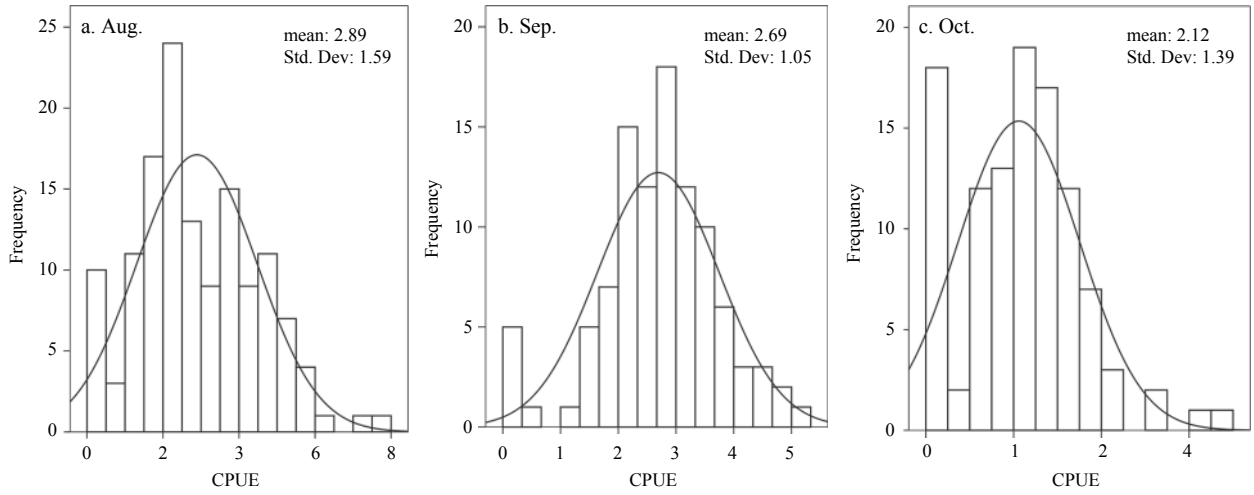

Fig. 2. The distributions of CPUE at 30′×30′ for *O. bartramii* CPUE in the northwest Pacific Ocean.

Table 2. Scaling equations and goodness-of-fit R^2s of entire fishery data of each month for *O. bartramii* in the northwest Pacific Ocean

Index	Month	Equation	R^2	Relation	Character
Max	Aug.	$y=6.120\,5+8.752\,4\exp(-0.061\,1x)$	0.861 6	exponential	decay
	Sep.	$y=5.166\,5+8.452\,7\exp(-0.062\,9x)$	0.775 4	exponential	decay
	Oct.	$y=10.582\,3-0.283\,4x+0.004\,3x^2$	0.824 3	quadratic polynomial	upward
		$y=76.356\,2-1.950\,1x+0.013\,1x^2$	0.901 7	quadratic polynomial	upward
CV	Aug.	$y=0.306\,9+0.290\,9\exp(-0.017\,7x)$	0.851 3	exponential	decay
	Sep.	$y=0.414\,5+0.125\,3\exp(-0.976\,7x)$	0.707 7	exponential	decay
	Oct.	$y=0.665\,3-0.007\,2x+0.000\,2x^2$	0.766 4	quadratic polynomial	upward
		$y=3.642\,7-0.080\,3x+0.000\,5x^2$	0.886 0	quadratic polynomial	upward

Note: y represents the summary statistics and x the spatial scale measured in minutes (hereinafter the same).

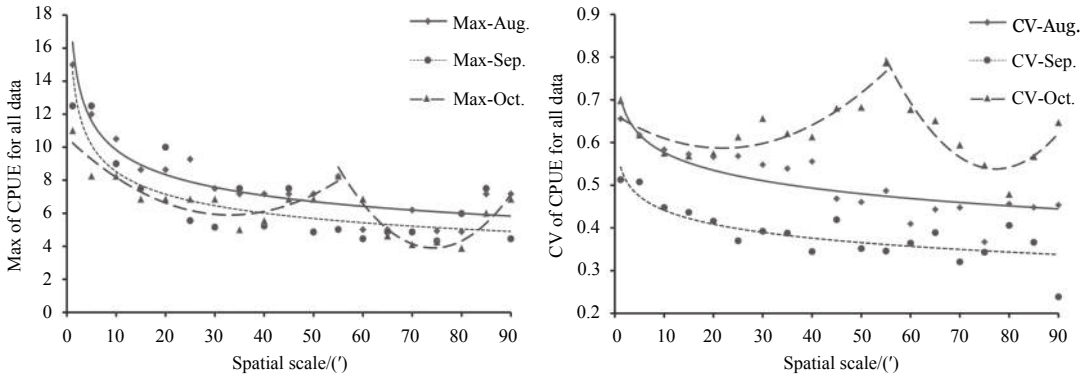

Fig. 3. Scaling relations of Max and CV of CPUE for *O. bartramii* in the northwest Pacific Ocean.

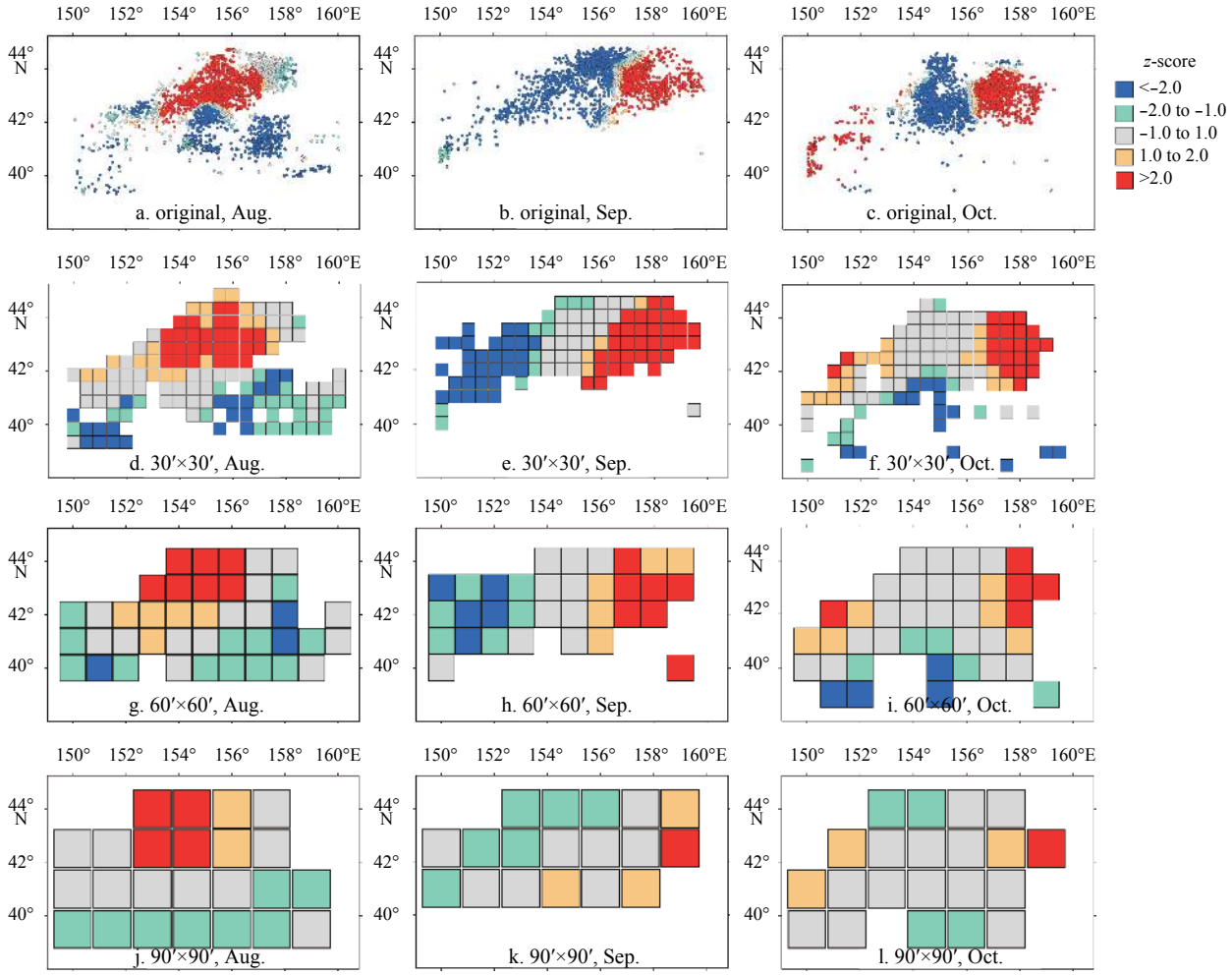

Fig. 4. The spatial hotspots of *O. bartramii* in the northwest Pacific Ocean at original, 30′×30′, 60′×60′ and 90′×90′ scales.

with changing scales. The CV for August and September showed a consistent lowering variation for *O. bartramii* CPUE as the spatial scale became coarser, while the CV for October is more complex.

3.3 *Scale impacts on summary statistics for hot/cold spots*

Spatial hot and cold spots were identified for all three months, as illustrated by the local clusters at four spatial scales including original, 30′×30′, 60′×60′, and 90′×90′ (Fig. 4). One hot and two cold spots were identified for August at the original scale, one hot and one cold spots were identified for September, and two hot and one cold spots were identified for October. The tessellations at 30′×30′ and 60′×60′ scales showed the same results, but the shapes differ between spatial scales. No cold spot was identified for any fishery data at coarse spatial scales from 80′ to 90′. The locations of both hot and cold spots moved slightly with changing scales. Points with *z*-score ranging from –1 to 1 (indicating spatial random patterns of CPUE) increased significantly as the spatial scale became coarser. In other words, the spatial patterns of CPUE were homogenized as spatial scale became coarser.

Table 3. Scaling equations and goodness-of-fit R^2s of spatial hot and cold spots for *O. bartramii* in the northwest Pacific Ocean

Cluster	Index	Month	Equation	R^2	Relation	Character
Hot spot	Max	Aug.	y=13.378–0.240 1x+0.001 9x^2	0.853 0	quadratic polynomial	upward
		Sep.	y=12.373–0.268 5x+0.002 4x^2	0.763 6	quadratic polynomial	upward
		Oct.	y=10.418–0.246x+0.003x^2	0.830 7	quadratic polynomial	upward
	SD	Aug.	y=2.234 1–0.053 8x+0.000 5x^2	0.775 8	quadratic polynomial	upward
		Sep.	y=1.516 8–0.025 1x+0.000 2x^2	0.667 0	quadratic polynomial	upward
		Oct.	y=1.601–0.415x+0.000 8x^2	0.758 1	quadratic polynomial	upward
	CV	Aug.	y=0.512–0.012 8x+0.000 1x^2	0.845 7	quadratic polynomial	upward
		Sep.	y=0.489 7–0.009 4x+8×10$^{-5}x^2$	0.801 0	quadratic polynomial	upward
		Oct.	y=0.582 4–0.018 3x+0.000 3x^2	0.919 8	quadratic polynomial	upward
	kurtosis	Aug.	y=4.170 1–0.025 4x	0.612 9	linear	decay
		Sep.	y=6.648 6exp(–0.02x)	0.783 4	exponential	decay
		Oct.	y=5.830 4exp(–0.015x)	0.718 9	exponential	decay
	Q1	Aug.	y=2.403$x^{0.143\,9}$	0.914 0	power law	growth
		Sep.	y=1.651 6$x^{0.188\,6}$	0.860 7	power law	growth
		Oct.	y=1.564 2$x^{0.161\,5}$	0.860 7	power law	growth
	median	Aug.	y=1.651 6$x^{0.188\,6}$	0.754 1	power law	growth
		Sep.	y=1.564 2$x^{0.161\,5}$	0.800 1	power law	growth
		Oct.	y=2.739 8+0.015 1x	0.755 5	linear	growth
Cold spot	mean	Aug.	y=2.725 6–0.029 8x+0.000 2x^2	0.882 9	quadratic polynomial	upward
		Sep.	y=2.717 8–0.028 6x+0.000 2x^2	0.798 1	quadratic polynomial	upward
		Oct.	y=2.223 8–0.074 5x+0.000 7x^2	0.974 4	quadratic polynomial	upward
	Max	Aug.	y=1.690 6+11.555 4exp(–0.068 7x)	0.964 5	exponential	decay
		Sep.	y=2.600 9+11.005 3exp(–0.065 3x)	0.953 7	exponential	decay
		Oct.	y=0.642 8+9.381 5exp(–0.067 9x)	0.985 8	exponential	decay
	SD	Aug.	–	–	–	–
		Sep.	y=1.6–0.020 8x+0.000 1x^2	0.749 9	quadratic polynomial	upward
		Oct.	y=1.537–0.040 6x+0.000 4x^2	0.977 6	quadratic polynomial	upward
	skewness	Aug.	y=1.729 9–0.047 2x+0.000 4x^2	0.728 7	quadratic polynomial	upward
		Sep.	y=1.130 5–0.040 8x+0.000 7x^2	0.811 4	quadratic polynomial	upward
		Oct.	y=1.285 4–0.069 4x+0.000 6x^2	0.888 2	quadratic polynomial	upward
	kurtosis	Aug.	y=8.272 6–0.252 7x+0.002 2x^2	0.820 7	quadratic polynomial	upward
		Sep.	y=7.088 4–0.213 5x+0.002 0x^2	0.879 2	quadratic polynomial	upward
		Oct.	y=4.490 3–0.115 3x+0.001 1x^2	0.780 1	quadratic polynomial	upward
	Q3	Aug.	y=2.938 9–0.055 6x+0.000 6x^2	0.766 9	quadratic polynomial	upward
		Sep.	y=3.365 1–0.02x+0.000 1x^2	0.747 6	quadratic polynomial	upward
		Oct.	y=3.098 4–0.087 8x+0.000 8x^2	0.980 4	quadratic polynomial	upward

The results show that the scaling relationships of hot spots differ from those of cold spots (Table 3, Figs 5 and 6). For hot spots, clear scaling relationships were identified for six of the summary statistics including Max, SD, CV, kurtosis, Q1 and median (Table 3 and Fig. 5) while no clear scaling relationships were identified for the remaining statistics such as Min, mean, skewness and Q3. There are only two statistics (CV for October and Q1 for August) with goodness-of-fit R^2s exceeding 0.9, two statistics (SD for September and kurtosis for August) with R^2s smaller than 0.7, while the remaining statistics have R^2s between 0.7-0.9. The scaling relationships for the hot spots define four general categories: (1) quadratic polynomial relationships that open upward for Max, SD and CV; (2) exponential relationships with a decaying trend for kurtosis in September and October; (3) linear relationships with a decaying trend for kurtosis in August and linear relationships with a growing trend for median in October; and (4) power law relationships with a growing trend for Q1 for all three months and for median in August and September. The Max value decreased before the nadirs but increased after the nadirs with changing spatial scales. The CV showed a lowering variation for *O. bartramii* CPUE before the nadirs but an increasing variation after the nadirs, as the spatial scale became coarser. CPUE kurtosis changed from leptokurtic to platykurtic with increasingly coarser spatial scales. Moreover, both Q1 and median indicate a general increase of CPUE for hot spots, as the spatial scale became coarser. This also indicates that these two statistics were highly sensitive to the change of the spatial scales.

For cold spots, clear scaling relationships were identified for six of the summary statistics including mean, Max, SD, skewness, kurtosis and Q3 (Table 3 and Fig. 6) while no clear scaling relationships were identified for the remaining statistics such as Min, CV, Q1 and median. Goodness-of-fit R^2s exceed 0.7 except SD in August; its R^2s is small and does not exhibit a clear scaling relationship (Fig. 6). The scaling relationships for the spatial cold spots come in two general categories: (1) a quadratic polynomial relationship that opens upward for mean, SD, skewness, kurtosis and Q3; and (2) an exponential relationship with a decaying trend for Max. The mean, SD, skewness, kurtosis and Q3 statistics decrease before the nadirs and increase after the nadirs. The SD for September and October showed that a decreasing trend and the CPUE values tend to be close to the mean. Skewness for September and October was positive but the left-skew was in-

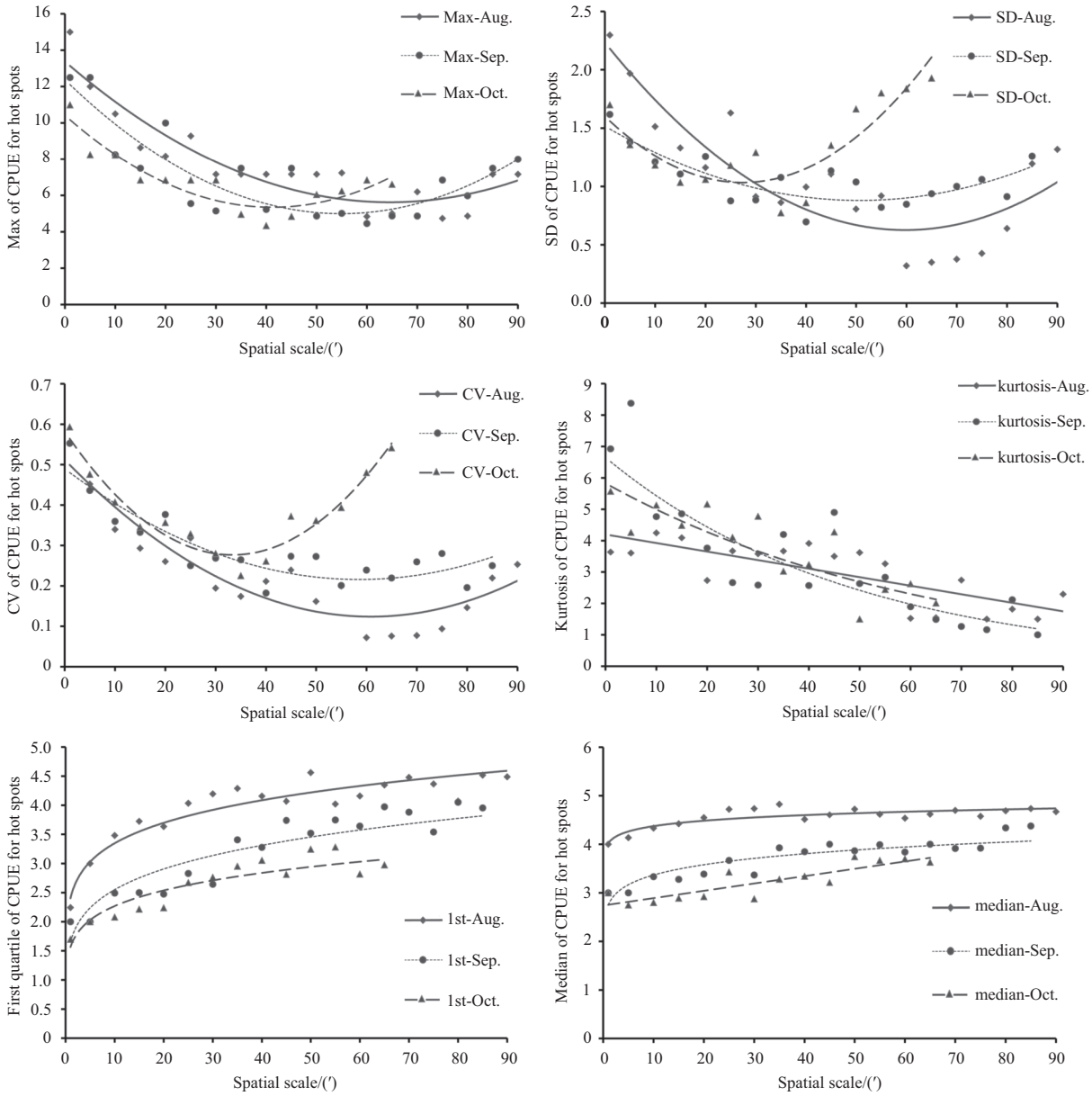

Fig. 5. Scale impacts on statistics of spatial hot spots for *O. bartramii* in the northwest Pacific Ocean.

creasingly weaker while it changed from left-skew to right-skew for August as the spatial scale became coarser. Kurtosis for August and September is larger than 3 at scales finer than 30′, indicating that the CPUE of cold spots yielded leptokurtic distributions; in contrast, the CPUE yielded platykurtic distributions at a scale coarser than 30′. For October, only scales finer than 20′ showed leptokurtic distributions. In addition, Q3 showed that CPUE decreases before the nadirs while it increases after the nadirs with the changing scales. Generally, the distribution of CPUE tends to be increasingly asymmetric and platykurtic as the spatial scale becomes coarser.

3.4 *Scale impacts on centroids of hot/cold spots*

The location of hot and cold spots as represented by their centroids is significantly affected by spatial scale (Fig. 7). For hot and cold spots, the centroids are close to each other at scales finer than 30′ while they vary in location at scales coarser than 30′. The centroid of the hot spot in August moved within a region about 2°×2° at scales finer than 60′, while it shifted over larger distances at scales coarser than 60′. For September, the centroid of the hot spot moved only about 60′ at scales finer than 30′ but fluctuated more widely at scales coarser than 30′. For October, the centroid moved along a line with a southwest-northeast direction at scales finer than 60′, but was significantly redistributed to the far west and east of the study area at scales coarser than 60′. The centroid of the cold spot in August does not move significantly at scales finer than 25′ but fluctuates more widely at coarser scales, especially above 60′. The centroid in September moved from the center (about longitude 155°E) to the west (about longitude 151°E), while the centroid in October moved from the north (latitude 41°N) to the south (latitude 39°N).

4 Discussion

Scaling issues are critical in identifying global and local spatial patterns in fisheries (Ciannelli et al., 2008). Multi-scale analysis has proven effective in addressing scaling issues in land-

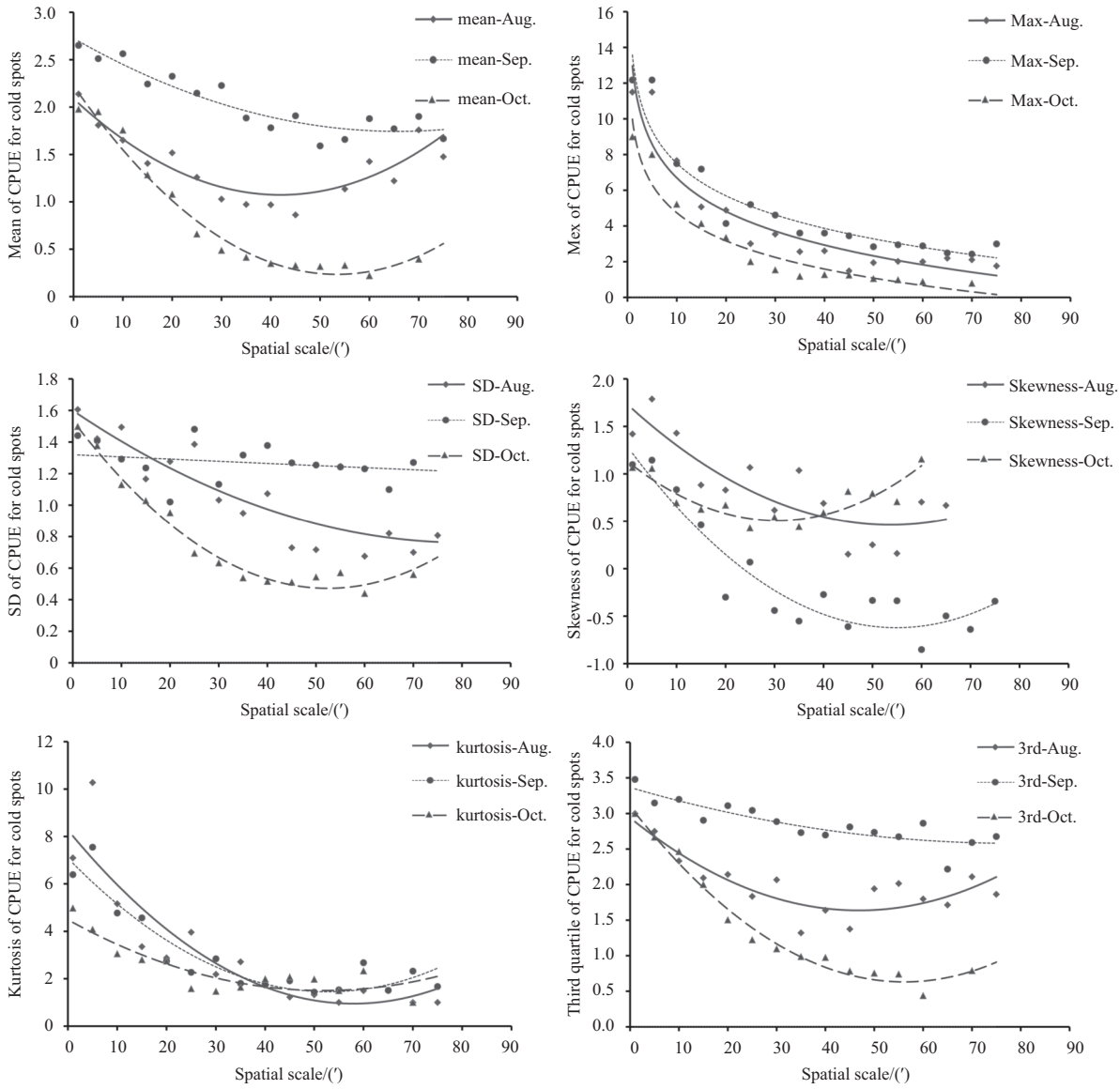

Fig. 6. Scale impacts on statistics of spatial cold spots for *O. bartramii* in the northwest Pacific Ocean.

scapes, in geography and in pelagic fisheries (Feng et al., 2016; Turner et al., 1989; Wu, 2004). We examined the scaling relations and scale effects of local spatial patterns of fisheries, using nominal CPUE data of *O. bartramii* in the northwest Pacific Ocean. As revealed in a previous study (Feng et al., 2016) and in this research, global and local spatial patterns such as clustering are significantly affected by spatial scale. We have identified scaling relationships for global spatial patterns of fisheries for *O. bartramii* in the northwest Pacific Ocean that include linear, logarithmic, exponential, power law, polynomial and descriptive functions. Logarithmic and descriptive relationships were not identified in local spatial patterns for *O. bartramii* based on the same fishery data.

For all data, the spatial indices (Feng et al., 2016) have clearer scaling relationships than do the summary statistics (c.f. Table 2 and Fig. 3). The spatial indices are therefore more appropriate as indicators of the optimum scale and coarsest allowable scale for conducting spatial analyses. The goodness-of-fit R^2s for the local spatial patterns are small when compared to the global patterns, indicating that the local patterns showed a slightly less strong regularity for scaling. In other words, the scaling relationships and scale effects of local spatial patterns are more complex. Our previous research showed that the non-zero CPUE data points (the Count index) yield power law scaling relationships and that the fractal dimensions of the scale effects were 2.224, 2.265, 2.268 for August, September and October, successively (Feng et al., 2016). We did not conduct a detailed analysis of scaling relations for Count index of hot and cold spots in this research. A brief examination of Count index change showed that the fractal dimensions are 2.487, 2.379 and 2.751 for hot spots for August, September and October, successively, and are 2.593, 2.529 and 2.539 for cold spots for the same three months. This suggests that the hot and cold spots are more sensitive to spatial scales as compared to the entire fishery data, because the former have larger fractal dimensions. The Count index is closely associated with the areas of hot and cold spots, however, the scaling relationship are more difficult to obtain when there are fewer data within the hot and cold spots of *O. bartramii*.

We identified hot and cold spots at a 0.05 significance level, but 0.01 has been used in previous research. We speculate that

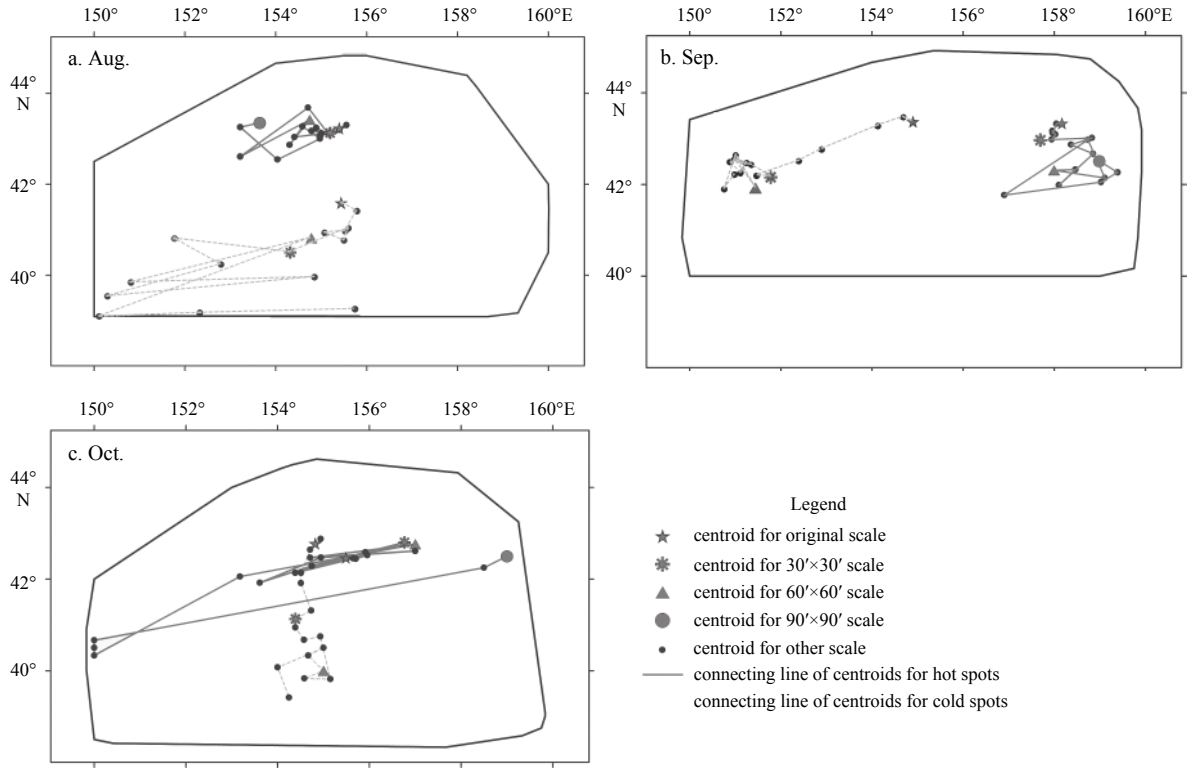

Fig. 7. Trajectories of centroids of spatial hot and cold spots across spatial scales.

the scaling relationships are similar at 0.01 significance, but the areas of the hot and cold spots would be smaller, and the cold spots would disperse on a less coarse scale. From the centroid perspective, the hot and cold spot locations at scales coarser than 30′ usually differ significantly from those at the original scale. It is therefore not advisable to identify the local spatial patterns of fisheries using this scale. Anselin Local Moran's I can be used to explore the statistically significant spatial clusters, i.e., hot and cold spots (Anselin, 1995, 2004). The impact of scale on clusters of Anselin Local Moran's I is not discussed in this paper, but the scaling relationships and scale effects are probably similar to those for the hot/cold spots derived using Getis-Ord Gi*. Spatial K-means can also identify spatial clusters of fisheries but these clusters are not necessarily associated with the hot/cold spots (Jain, 2010; Mullon et al., 2005). As such, the scale impacts on the spatial clusters derived using spatial K-means may be quite different from those based on Getis-Ord Gi* and Anselin Local Moran's I.

We speculate that in some pelagic fisheries such as *Dosidicus gigas*, *Thunnus albacares* and *Katsuwonus pelamis*, the scaling relationships are more complex because there are fewer commercial fishing records for these species as compared to *O. bartramii*. For example, commercial fishery data of *K. pelamis* are usually available at a coarse 1° spatial scale; as a consequence, multi-scale analysis may not be accurate and/or informative. The jumbo flying squid (*D. gigas*) is a fast-growing and short-lived species similar to *O. bartramii*. Its population is usually composed of individuals who have the capacity to migrate both vertically and horizontally in respond to changing environments (Arkhipkin and Murzov, 1986; Chen and Chiu, 2003; Yu et al., 2016b).

This study examined the impacts of changing spatial scales on spatial hot and cold spots for *O. bartramii* in the northwest Pacific Ocean. It extends the work of Feng et al. (2016) and describes the scale impacts on local clusters by considering several statistics including mean, SD, CV, skewness, kurtosis, Q1, median, Q3, area and centroid. The scale impacts were assessed in accordance with the linear, exponential, power law, and polynomial functions as commonly reported in landscape ecology (Turner et al., 1989; Wu, 2004) and more recently in fisheries (Feng et al., 2016).

It should be noted that the specific parameters of the scaling formula may not be applicable to other pelagic fisheries because they were affected by the selection of fishery dataset, but the scaling relations of spatial hotspots are appropriate to other fast-growing and short-lived species. Meanwhile, the methods presented in this paper are widely applicable to analyses of the spatial scale effects for any other commercial species. Our results contribute to a better understanding of the relationships between spatial scale and local spatial clusters in fisheries and in selection of the appropriate spatial scale for spatial analysis in fisheries.

References

Anselin L. 1995. Local indicators of spatial association-LISA. Geogr Anal, 27(2): 93–115

Anselin L. 2004. Exploring spatial data with GeoDa™: a workbook. Urbana, USA: University of Illinois, 61801

Arkhipkin A I, Murzov S A. 1986. Age and growth patterns of dosidicus gigas (Ommastrephidae). In: Ivanov B G, ed. Present State of Fishery for Squids and Prospects of Its Development. Moscow: VNIRO Press, 107–123

Carocci F, Bianchi G, Eastwood P, et al. 2009. Geographic Information Systems to Support the Ecosystem Approach to Fisheries: Status, Opportunities and Challenge. Rome, Italy: Food and Agriculture Organization of the United Nations

Chen Xinjun, Chen Yong, Tian Siquan, et al. 2008. An assessment of the west winter–spring cohort of neon flying squid (*Ommastre-*

phes bartramii) in the Northwest Pacific Ocean. Fish Res, 92(2–3): 221–230
Chen C S, Chiu T S. 2003. Variations of life history parameters in two geographical groups of the neon flying squid, *Ommastrephes bartramii*, from the North Pacific. Fish Res, 63(3): 349–366
Chen Xinjun, Tian Siquan, Guan Wenjian. 2014. Variations of oceanic fronts and their influence on the fishing grounds of *Ommastrephes bartramii* in the Northwest Pacific. Acta Oceanol Sin, 33(4): 45–54
Ciannelli L, Fauchald P, Chan K S, et al. 2008. Spatial fisheries ecology: Recent progress and future prospects. J Mar Syst, 71(3–4): 223–236
Cope J M, Punt A E. 2011. Reconciling stock assessment and management scales under conditions of spatially varying catch histories. Fish Res, 107(1–3): 22–38
Ebdon D. 1985. Statistics in Geography: A Practical Approach. 2nd ed. London: Wiley-Blackwell
Feng Yongjiu, Chen Xinjun, Liu Yan. 2016. The effects of changing spatial scales on spatial patterns of CPUE for *Ommastrephes bartramii* in the northwest Pacific Ocean. Fish Res, 183: 1–12
Feng Yongjiu, Chen Xinjun, Liu Yan. 2017a. Detection of spatial hot spots and variation for the neon flying squid *Ommastrephes bartramii* resources in the northwest Pacific Ocean. Chin J Oceanol Limnol, 35(4): 921–935
Feng Yongjiu, Chen Xinjun, Yang Liu. 2017b. Examining spatiotemporal distribution and CPUE-environment relationships for the jumbo flying squid *Dosidicus gigas* offshore Peru based on spatial autoregressive model. Chin J Oceanol Limnol: doi: 10.1007/s00343-018-6318-3
Feng Yongjiu, Cui Li, Chen Xinjun, et al. 2017c. A comparative study of spatially clustered distribution of jumbo flying squid (*Dosidicus gigas*) offshore Peru. J Ocean Univ China, 16(3): 490–500
Feng Yongjiu, Liu Yan. 2015. Fractal dimension as an indicator for quantifying the effects of changing spatial scales on landscape metrics. Ecol Indic, 53: 18–27
Fosså J H, Mortensen P B, Furevik D M. 2002. The deep-water coral *Lophelia pertusa* in Norwegian waters: distribution and fishery impacts. Hydrobiologia, 471(1–3): 1–12
Gao Feng, Chen Xinjun, Guan Wenjiang, et al. 2016. A new model to forecast fishing ground of *Scomber japonicus* in the Yellow Sea and East China Sea. Acta Oceanol Sin, 35(4): 74–81
Getis A, Aldstadt J. 2010. Constructing the spatial weights matrix using a local statistic. In: Anselin L, Rey S J, eds. Perspectives on Spatial Data Analysis. Berlin, Heidelberg: Springer, 147–163
Getis A, Ord J K. 1996. Spatial analysis and modeling in a GIS environment. In: McMaster R B, Lynn Usery E, eds. A Research Agenda for Geographic Information Science. Boca Raton: CRC Press, 157–196
Gilly W F, Markaida U, Baxter C H, et al. 2006. Vertical and horizontal migrations by the jumbo squid *Dosidicus gigas* revealed by electronic tagging. Mar Ecol Prog Ser, 324: 1–17
Gong Caixia, Chen Xinjun, Gao Feng, et al. 2014. Effect of spatial and temporal scales on habitat suitability modeling: A case study of *Ommastrephes bartramii* in the northwest pacific ocean. J Ocean Univ China, 13(6): 1043–1053
Guinet C, Dubroca L, Lea M A, et al. 2001. Spatial distribution of foraging in female Antarctic fur seals *Arctocephalus gazella* in relation to oceanographic variables: a scale-dependent approach using geographic information systems. Mar Ecol Prog Ser, 219: 251–264
Gutiérrez N L, Masello A, Uscudun G, et al. 2011. Spatial distribution patterns in biomass and population structure of the deep sea red crab *Chaceon notialis* in the Southwestern Atlantic Ocean. Fish Res, 110(1): 59–66
Harford W J, Ton C, Babcock E A. 2015. Simulated mark-recovery for spatial assessment of a spiny lobster (*Panulirus argus*) fishery. Fish Res, 165: 42–53
Huang Jiansheng, Sun Yao, Jia Haibo, et al. 2014. Spatial distribution and reconstruction potential of Japanese anchovy (*Engraulis japonicus*) based on scale deposition records in recent anaerobic sediment of the Yellow Sea and East China Sea. Acta Oceanol Sin, 33(12): 138–144
Jain A K. 2010. Data clustering: 50 years beyond K-means. Pattern Recogn Lett, 31(8): 651–666
Jennings S, Kaiser M, Reynolds J D. 2009. Marine Fisheries Ecology. New York: John Wiley & Sons
Jiang Tao, Chai Chai, Wang Jifang, et al. 2016. Temporal and spatial variations of abundance of phycocyanin- and phycoerythrin-rich *Synechococcus* in Pearl River Estuary and adjacent coastal area. J Ocean Univ China, 15(5): 897–904
Meaden G J, Aguilar-Manjarrez J. 2013. Advances in Geographic Information Systems and Remote Sensing for Fisheries and Aquaculture. Roma, Italy: Food and Agriculture Organization of the United Nations
Mitchell A. 2005. The ESRI Guide to GIS Analysis, Volume 2: Spatial Measurements and Statistics. Redlands, CA: Esri Press
Mullon C, Fréon P, Cury P. 2005. The dynamics of collapse in world fisheries. Fish Fish, 6(2): 111–120
Nishida T, Chen Dinggeng. 2004. Incorporating spatial autocorrelation into the general linear model with an application to the yellowfin tuna (*Thunnus albacares*) longline CPUE data. Fish Res, 70(2–3): 265–274
Ord J K, Getis A. 1995. Local spatial autocorrelation statistics: Distributional issues and an application. Geogr Anal, 27(4): 286–306
Paulino C, Segura M, Chacón G. 2016. Spatial variability of jumbo flying squid (*Dosidicus gigas*) fishery related to remotely sensed SST and chlorophyll-a concentration (2004–2012). Fish Res, 173: 122–127
Peeters A, Zude M, Käthner J, et al. 2015. Getis–Ord's hot-and cold-spot statistics as a basis for multivariate spatial clustering of orchard tree data. Comput Electron Agr, 111: 140–150
Saul S E, Walter III J F, Die D J, et al. 2013. Modeling the spatial distribution of commercially important reef fishes on the West Florida Shelf. Fish Res, 143: 12–20
Su N J, Sun C L, Punt A E, et al. 2008. Environmental and spatial effects on the distribution of blue marlin (*Makaira nigricans*) as inferred from data for longline fisheries in the Pacific Ocean. Fish Oceanogr, 17(6): 432–445
Swartz W, Sala E, Tracey S, et al. 2010. The spatial expansion and ecological footprint of fisheries (1950 to present). PLoS One, 5(12): e15143
Tian Siquan, Chen Yong, Chen Xinjun, et al. 2010. Impacts of spatial scales of fisheries and environmental data on catch per unit effort standardisation. Mar Freshwater Res, 60(12): 1273–1284
Turner M G, O'Neill R V, Gardner R H, et al. 1989. Effects of changing spatial scale on the analysis of landscape pattern. Landscape Ecol, 3(3–4): 153–162
Wiens J A. 1989. Spatial scaling in ecology. Func Ecol, 3(4): 385–397
Wu Jianguo. 2004. Effects of changing scale on landscape pattern analysis: scaling relations. Landscape Ecol, 19(2): 125–138
Xu Jie, Chen Xinjun, Chen Yong, et al. 2016. The effect of sea surface temperature increase on the potential habitat of *Ommastrephes bartramii* in the Northwest Pacific Ocean. Acta Oceanol Sin, 35(2): 109–116
Yang Mingxia, Chen Xinjun, Feng Youjiu, et al. 2013. Spatial variability of small and medium scales, resource abundance of *Ommastrephes bartramii* in Northwest Pacific. Haiyang Xuebao (in Chinese), 33(20): 6427–6435
Yu Wei, Chen Xinjun, Chen Yong, et al. 2015. Effects of environmental variations on the abundance of western winter-spring cohort of neon flying squid (*Ommastrephes bartramii*) in the Northwest Pacific Ocean. Acta Oceanol Sin, 34(8): 43–51
Yu Wei, Chen Xinjun, Yi Qian, et al. 2016a. Spatio-temporal distributions and habitat hotspots of the winter–spring cohort of neon flying squid *Ommastrephes bartramii* in relation to oceanographic conditions in the Northwest Pacific Ocean. Fish Res, 175: 103–115
Yu Wei, Yi Qian, Chen Xinjun, et al. 2016b. Modelling the effects of climate variability on habitat suitability of jumbo flying squid, *Dosidicus gigas*, in the Southeast Pacific Ocean off Peru. ICES J Mar Sci, 73(2): 239–249